Available online at www.sciencedirect.com
SCIENCE DIRECT
Earth and Planetary Science Letters 241 (2006) 454–465
EPSL
www.elsevier.com/locate/epsl

Fluid flow through rough fractures in rocks. II: A new matching model for rough rock fractures

Steven R. Ogilvie [a,b,*], Evgeny Isakov [a], Paul W.J. Glover [a,c]

[a] Department of Geology and Petroleum Geology, University of Aberdeen, Aberdeen AB24 3UE, Scotland, UK
[b] BP Exploration Ltd, Farburn Industrial Estate, Dyce, Aberdeen, Scotland, UK
[c] Département de Géologie et de Génie Géologique, Faculté des Sciences et de Genie, Université Laval Sainte-Foy, Québec, Canada G1K 7P4

Received 10 May 2005; received in revised form 21 November 2005; accepted 29 November 2005
Available online 4 January 2006
Editor: E. Boyle

Abstract

An understanding of fluid flow through natural fractures in rocks is important in many areas, such as in the hydrocarbon and water industries, and in the safe design of disposal sites for domestic, industrial and nuclear waste. It is often impractical to obtain this information by field or laboratory scale measurements, so numerical modelling of fluid flow must be carried out using synthetic fractures with rough fracture surfaces that are representative of the natural rock fractures. Clearly there are two practical requirements; (i) the development of a method for analysing natural rock fractures to obtain their characteristic parameters, and (ii) the development of techniques for creating high quality synthetic fractures using these parameters. We have implemented these practical requirements in two new software packages. The first, ParaFrac allows the analysis and parameterisation of fracture surfaces and apertures. The second, SynFrac, enables the numerical synthesis of fracture surfaces and apertures with basic prescribed parameters. Synthetic fractures are created using, (i) a new model, which takes full account of the complex matching properties of fracture surfaces using two new parameters, a minimum matching fraction and a transition length and (ii) an improved method of partially correlated random number generation. This model more closely captures the often complex matching properties of real rock fractures than previous more simplified models.

Keywords: fluid flow; rough fractures; synthetic fractures; apertures

1. Introduction

An understanding of fluid flow through natural fractures in rocks is important in many areas, such as in the hydrocarbon and water industries [1], and in the safe design of disposal sites for domestic, industrial and nuclear waste [2]. It is often impractical to obtain this information by field or laboratory scale measurements, so numerical modelling of fluid flow must be carried out. Such models must include the effect of the rough fracture surfaces (i.e., fracture aperture variation), on the fluid flow if they are to be considered to be effective (e.g., [3–15]).

Numerical synthetic fractures used in the modelling of rough fractures need to fulfil two main criteria. First, they should be representative of the natural rock fractures (i.e., they must be tuned to have the same basic parameters as the natural fractures, including surface and aperture fractal dimensions, surface asperity height

* Corresponding author. BP Exploration Ltd, Farburn Industrial Estate, Dyce, Aberdeen, UK.
E-mail address: steven.ogilvie@bp.com (S.R. Ogilvie).

0012-821X/$ - see front matter © 2005 Elsevier B.V. All rights reserved.
doi:10.1016/j.epsl.2005.11.041

distributions, aperture distributions, anisotropies, and matching characteristics). Second, for accurate numerical modelling, a suite of fractures should be used, each of which have the same basic parameters, but differ in their actual physical topographies [11–13].

However, natural fractures in rocks are complicated by two phenomena. The first, anisotropy, is difficult to measure quantitatively without robust methodologies, which have not, to our knowledge, been reported previously in the geophysical literature. The second is the degree of correlation between two rough rock fracture surfaces that occurs at long wavelengths. This correlation is zero at short wavelengths, where the two surfaces are independent of each other, and increases gradually with increasing wavelength until a maximum degree of correlation is attained [3,16–21]. Brown and Scholz [18] and Power and Tullis [22] found that surfaces are well correlated above the scale of a few millimeters. In between, the degree of correlation must vary, but currently it is unknown for any given rock what function describes this gradational behaviour.

This correlation is often called "matching" (Fig. 1a). However, since the correlation is between the power of Fourier components of the surface at any particular wavelength, the term is a little misleading, because it does not necessarily lead to perfectly matched fracture surfaces. Brown [4] recognised the difficulty, and used two different definitions of a so-called mismatch wavelength to define the wavelength, above which the fracture surfaces were "matched" (Fourier components had equal power and equivalent phase), and below which the fracture surfaces behaved completely independently. This scenario is described schematically in Fig. 1. Clearly, such a sudden cut-off is not realistic, as will be demonstrated later with data from real rock fractures. Glover et al. [8,9] recognised this and instituted a method that enabled a gradual linear change in the degree of correlation from no matching at (and below) a wavelength half of a defined characteristic mismatch wavelength (ML), to some fraction of complete matching occurring at the largest wavelength possible for the model (Fig. 1b). This method was an improvement upon the Brown [4] methodology, but still not flexible enough to take account of the variation in real rock fractures. Also, the method used by Glover et al. [8,9] to obtain partially correlated random deviates, which are central to this type of modelling, was not mathematically robust, leading to a non-uniform distribution of random deviates, and hence underestimated fracture apertures. The approach in this paper is to modify (and completely recode) the methods used by Glover et al. [8,9] to take account of both of these weaknesses and to make the model more generally applicable (Fig. 1c) [13].

2. Parameterisation of real rock fractures

Rough fracture surfaces and their resulting apertures are complex entities. Analysis has been carried out on a suite of five laboratory-induced Mode I fractures in rocks. These are (*xy*-size 100 × 100 mm) a (i) red granite (Norway) (ii) syenite (Sweden), (iii) gabbro (South Africa), (iv) medium-grained, durable sandstone (NE Scotland) and (v) granodiorite (Finland) (Fig. 2). These have very low matrix porosities and permeabilities, so the fracture may provide the only opportunity for fluid storage and flow. None of the samples is significantly anisotropic. However, the syenite (Fig. 2b) consists of coarse, parallel labradorite and mica laths, which define a more anisotropic fabric than the others. It splits more easily, producing a smoother surface with a lower fractal dimension. In general, the finer grained samples (sandstones and granodiorite) tend to produce rougher surfaces (Fig. 2). Resin replicas

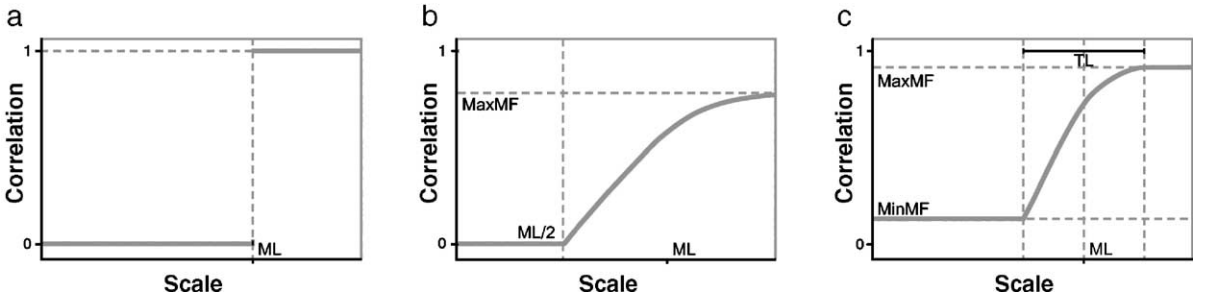

Fig. 1. Definitions of matching parameters. The definition of the mismatch parameters defined by Brown [4] (a), by Glover et al. [8,9] (b), and those used in this work (c), where, ML=mismatch wavelength, MFMAX=maximum matching fraction, MFMIN=minimum matching fraction and TL=transition length. Correlation is between the power of Fourier components of the surface at any particular wavelength. The phase part is controlled by random numbers, which depend upon the two original random number seeds and the matching parameters.

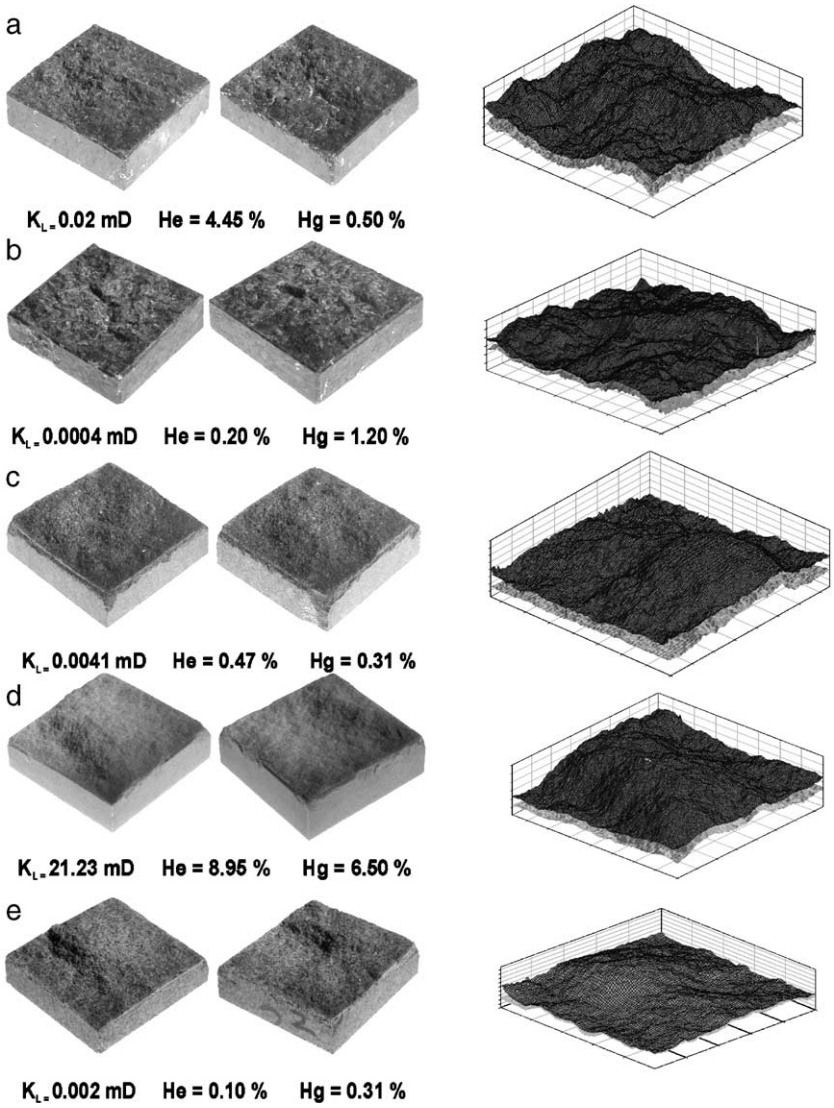

Fig. 2. Mode I rock fractures and respective surface topographies for (a) granite, (b) syenite, (c), gabbro, (d) sandstone, and (e) granodiorite. Matrix petrophysical data are given, where K_L=equivalent liquid permeability, He=helium technique porosity and Hg=mercury technique porosity.

of each surface were reproduced to within 1 μm and they were profiled using an optical method described in detail in Isakov et al. [12] and Ogilvie et al. [23].

In-house software, ParaFrac was used to perform statistical, spectral, correlative and fractal analyses of the profiled fracture surfaces and apertures, to determine their basic geometric, fractal, and matching parameters. The numerical analysis of rough fracture surfaces allows us to obtain a set of geometrical parameters that fully describe them. These parameters are useful in that they provide a method for numerically characterising fractures, allowing differences between fractures to be analysed quantitatively [13].

2.1. Fourier analyses

To a first approximation, all surfaces have a power spectral density function $G(k)$, of the form [28],

$$G(k) = Ck^{-\alpha} \quad (1)$$

where,

$k = 2\pi/\lambda$ Wavenumber
λ Wavelength or distance along the profile
C Proportionality constant (varies among surfaces)
α Power, falls in the range of $2 < \alpha < 3$

Fast Fourier Transforms (FFTs) were used to calculate and display the power spectral density (PSD) of the surfaces and their resulting aperture as a function of wavelength on log–log scales (where the wavenumber k, the wavelength λ and the frequency v of the Fourier components are related by $k=1/\lambda$ and $v=2\pi/\lambda$). Linear regression to the full PSD for the surfaces, and to the linear short wavelength portion of the aperture allow the fractal dimensions (measure of the scaling behaviour of the surface, containing information regarding the relative positions of asperities of different sizes) of the surfaces and the aperture to be calculated (e.g., [4,22,24]). Profiles of natural rock fractures have spectra with slopes between -2 and -3 corresponding to surface fractal dimensions of 2.5 to 2.0 respectively [4]. Our power density spectrum analysis was performed at a resolution of ~0.2 mm and 512 grid points for ~10 cm samples. The data were not resampled during the analyses, therefore we did not investigate how resampling affects the results. It is likely that this resolution is sufficient for "smooth" samples like the granite, and that no more information can be derived from the sample by increase of the resolution. On the other hand, fine grains of sandstone may be too small to be resolved at the resolution of 0.2 mm, so these data may have lower accuracy.

The anisotropy of fractal dimension of the surface (A_{sD}) allows the surface to have different fractal dimensions in different directions across the surface. This anisotropy and the resulting apertures were obtained by converting each fracture profile (of multiple, parallel cross-sections) into a spectrum separately, and then all the spectra were plotted on the same graph, giving a scattering pattern. The average spectrum was then calculated and the best-fit regression found.

2.2. Matching analyses

Fourier analysis was used to determine the matching properties of the fractures. This calculates the ratio of the PSDs from the aperture with the sum of the PSDs of the two surfaces composing the fracture and plots it as a function of wavelength on a log–log scale. We call this parameter the PSD Ratio (PSDR), where,

$$\mathrm{PSDR} = \mathrm{PSD(aperture)}/(\mathrm{PSD(upper\ surface)} + \mathrm{PSD(lower\ surface)}) \quad (2)$$

At small wavelengths (i.e., high frequencies and large wavenumbers) the PSDR tends to unity if the surfaces are completely independent [8,9]. This is because the fracture surfaces are not correlated point by point, and hence the powers of the Fourier components of the aperture are equal to the sum of those for each of the fracture surfaces. If the PSDR is less than unity, it shows that there is some matching occurring at the highest wavenumbers (smallest wavelengths) available in the data set. It can be seen, therefore that the PSDR at the highest wavenumber (smallest wavelength) of the data set $(\mathrm{PSDR})_{\mathrm{kmax}}=(1-\mathrm{MFMIN})$, and hence MFMIN can be obtained (Fig. 1). There is a gradual increase in matching of the two surfaces as the wavelength increases (i.e., the frequency and wavenumber decreases). As this occurs, the PSDR drops to values below unity, but never below zero. This is because there is increasing correlation between the two fracture surfaces that results in loss of power of the Fourier components of the aperture. Consequently, the PSDR at the highest wavelength of the data set $(\mathrm{PSDR})_{\mathrm{kmin}}=(1-\mathrm{MFMAX})$, and hence MFMAX can be obtained (Fig. 1). We define the mismatching wavelength (ML) for the system as the wavelength λ_{ML} (represented by the wavenumber k_{ML}, where $\lambda_{\mathrm{ML}}=1/k_{\mathrm{ML}}$), which lies equidistant between the wavelength at which minimum matching occurs and that at which maximum matching occurs in the data set (Fig. 1). Fig. 3 shows the same profile through 3D synthetic fractures with the same geometrical parameters but different mismatch wavelengths (ML). In Fig. 3a, the mismatch wavelength (ML) is greater than the maximum size of the fracture. In other words, the two surfaces are independent for all wavelengths represented in the fracture. This results in a large fracture aperture. Fig. 3b–d represent a gradual decrease in the mismatch wavelength (ML) such that it lies between the maximum size of the fracture and the Nyqvist wavelength [25] of the fracture (i.e., 1/512 (resolution of 512×512) the smallest spatial frequency that can be defined on a 1024×1024 grid)). As the mismatch wavelength decreases, more and more of the larger wavelengths that describe each surface are matched. The asperities associated with these wavelengths (which are relatively large due to the fractal scaling of the fracture surfaces) do not interact in order to hold the aperture wide open, but are matched such that the aperture "fits together" better. Hence the aperture decreases dramatically. Fig. 3e is the extreme case, where the mismatch wavelength (ML) is such that all wavelengths represented by the fracture are matched. As the two surfaces are now physically the same, the aperture has collapsed to zero.

The final parameter introduced into the new model is the transition length (TL). This is defined as the difference in wavelength between that at which maximum matching occurs and that at which minimum matching

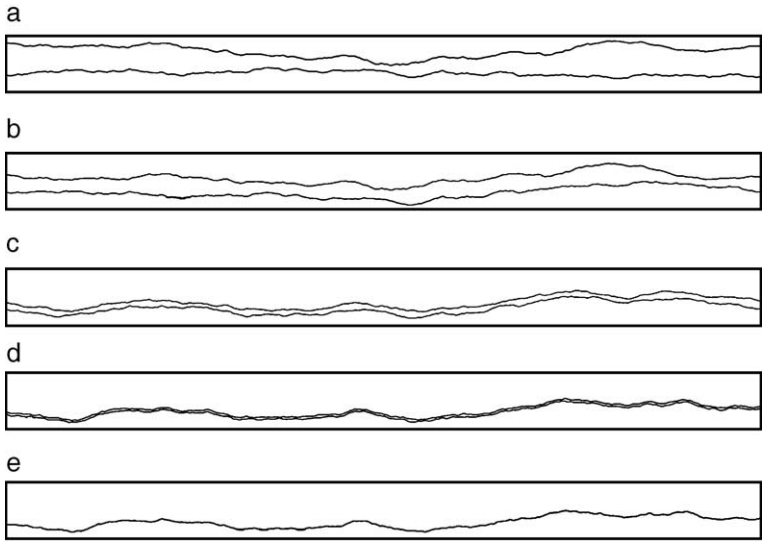

Fig. 3. Approaches to the controls on matching. (a) Largest fracture aperture resulting from the mismatch wavelength (ML) greater than maximum size of fracture, (b)–(d) apertures resulting from a gradual decrease in ML and (e) zero aperture where mismatch length is such that all wavelengths represented by the fracture are matched.

occurs, and corresponds to the width (expressed in wavelength) of the transition zone [13] (Fig. 1).

3. Creation of synthetic fractures

Clearly, there are limitations in terms of the amount of profiles, which can be produced. Therefore, combinations of numerical fractures with the same basic geometry but with different physical topographies were generated using SynFrac software [11,13]. The following parameters from the rock fractures (using ParaFrac) were required to create synthetic fractures, (i) physical size, (ii) mismatch length (ML), (iii) transition length (TL), (iv) standard deviation of surface heights, (v) anisotropy factor, (vi) fractal dimension (D_f), (vii) maximum matching fraction (MFMAX) and (viii) minimum matching fraction (MFMIN).

Fractures were produced using the Brown [4] method, Glover et al. [8,9] method, and our improved method of controlling the degree of fracture surface correlation with wavelength (e.g., [13]). Fracture surface generation is based upon the spectral synthesis method [4,17,26] on a grid up to 1024×1024 pixels and at any physical scale. The method differs slightly depending upon which type of matching approach is used. The following description is based upon the implementation of the new approach, and comments are added where the Brown [4] and Glover et al. [8,9] approaches differ from this.

The spectral synthesis method involves defining a symmetric matrix containing Fourier components. These Fourier components are calculated to obey the various parameters for the fracture. Each component has two parts; (i) the amplitude and (ii) the phase. The amplitude scales with a power law that contains the fractal dimension information, and any information about the relative anisotropy of surface heights. The phase part is controlled by random numbers, which depend in their turn upon the two original random number seeds and the matching parameters. Two random number seeds control the actual topographies of the two fracture surfaces, and therefore control the resulting aperture. We can create a suite of synthetic fractures, say 20, using 20 sets of two random numbers and one set of geometrical parameters derived from a natural fracture. The resulting 20 synthetic fractures will each share the same geometrical parameters as the original natural fracture, but they will be different physically.

The first step is to generate two matrices where each point in each matrix corresponds to that in the final matrix of Fourier components. These two matrices contain random numbers that are partially correlated to some degree. The degree of partial correlation depends upon the matching parameters. This step was not necessary for Brown [4], as he had only to choose which of the two random numbers to use. In fact, he generated one surface with one set of random numbers. He then generated a second fracture surface using (i) a different set of random numbers for the Fourier components corresponding to wavelengths that were less than the mismatch wavelength (ML), (i.e., where the

surfaces were independent), and (ii) the same random numbers that were used to generate the first fracture for the Fourier components corresponding to wavelengths that were greater than the mismatch wavelength (ML), (i.e., where the surfaces were perfectly matched).

The implementation of the Glover et al. [8,9] method required the use of two independent sets of random numbers for the wavelengths that are less than the half the mismatch wavelength (ML), but to generate and use partially correlated random numbers for wavelengths above this value. To do this they linearly mixed the two random number sets using a linear weighting, which varied from zero at half of the mismatch wavelength (ML) to some fraction less than unity representing the maximum matching fraction (MFMAX) at the largest wavelength contributing to the fracture. The Glover et al. [8,9] and our new method require pairs of random values (A, B) to be generated with a prescribed correlation coefficient, R. Glover et al. [8,9] proposed that,

$$B = RA + (1 - R)C, \tag{3}$$

where, A and C are two independent random values.

While this procedure does produce a partially correlated set of numbers (A, B), the target random value B is not uniformly distributed over the interval zero to unity. Hence, there is a fundamental fault in mixing random numbers this way. In fact, any simple algebraic mixing of sets of random numbers breaks the uniform distribution that was originally present in the two original random number data sets. We have overcome this problem by implementing a position swapping algorithm that enables a given mixing of two uniformly distributed random number data sets to be attained while retaining a uniform distribution in the final mixed and partially correlated random number data set. The algorithm is now described,

1. Two long ($>10^5$ numbers) sequences of independent random values, A, C, are generated.
2. The sequence of target random values, B is composed of the values in the sequence, C by re-arranging their order as follows,
   a. Sequence C is copied to B.
   b. Two numbers, B_n and B_m are randomly chosen in the sequence B. Their places are swapped if the correlation coefficient between A and B becomes close to the target value R after the swap.
   c. Step b is repeated as many times as is required in order to get the correlation between A and B equal to R with sufficient accuracy.
   d. Pairs (A_i, B_i) are used then as pairs of partially correlated random values.

An advantage is that the random sequence B has uniform distribution at probability. Also, this is a simple and elegant solution, but one that requires significant CPU time. Consequently, we use the improved method for creating partially correlated random number data sets to both the new matching approach and our improved implementation of the Glover et al. [8,9] approach. Also, the algorithm is not very economical as long sequences of random values are required and it may be inappropriate when just a few pairs of random values are necessary to generate the fracture. The implementation of the algorithm in SynFrac generates approximately 100 times more random values than it actually uses.

There is no evidence that an auto correlation is not introduced in the sequence B when swapping the values in the sequence. We can, however, state that,

a. When the correlation is low ($R \sim 0$), the sequence B is close to the sequence C, which is not auto correlated.
b. When the correlation is high ($R \sim 1$), the sequence B approaches the sequence A, which is not auto correlated.

The random number data sets are used to define the phase of the Fourier components. The fractal dimension and anisotropy are used to define the amplitude of the Fourier components. When all the Fourier components are known and arranged in a 2D complex and symmetric matrix, they are submitted to a 2D Fast Fourier Transform (FFT), the real part of which is the fracture surface with a mean value of zero. It only remains then to scale the surface to the required physical size, to scale the asperities to the size defined by the standard deviation of surface heights, and to shift the mean level of the fracture surface to whatever is required.

4. Results

There were two fracture surface positioning tasks. The first was an approximate positioning using OptiProf as reported in Isakov et al. [12]. The second was an automatic fine positioning performed in ParaFrac. It is not a problem if several possible relative positions of the surfaces that are close to each other have similar best-fits as there will always be a best one. The best matching position could be found without any problem and corresponds to a minimal mean aperture of the fracture.

The statistical properties of the 5 samples (Fig. 2) gathered by ParaFrac are given in Table 1. The para-

Table 1
Rock fractures tested with the new method

Parameter	*a*	b	c	d	e
Surface parameters					
Standard deviation (upper), ${}_{U}\sigma_s$ (mm)	1.97	1.89	1.82	2.82	3.17
Standard deviation (lower), ${}_{L}\sigma_s$ (mm)	2.07	2.03	2.07	3.24	3.25
Variance (upper), ${}_{U}\sigma_s^2$ (mm^2)	3.88	3.57	3.31	7.95	10.0
Variance (lower), ${}_{L}\sigma_s^2$ (mm^2)	4.28	4.12	4.28	10.5	10.6
Fractal dimension (upper), ${}_{U}D_f$ (–)	2.25	2.17	2.25	2.32	2.18
Fractal dimension (lower), ${}_{L}D_f$ (–)	2.16	2.18	2.22	2.23	2.22
Anisotropy in fractal dimension (upper), ${}_{U}A_{sD}$ (–)	0.88	1.04	1.42	1.07	1.16
Anisotropy in fractal dimension (lower), ${}_{L}A_{sD}$ (–)	0.86	0.97	1.41	1.08	1.20
Physical size, L (mm)	95.9	96.8	100	100	97.0
Measurement points per fracture size (–)	512	480	500	499	501
Resolution (μm)	190	200	200	200	190
Fracture parameters					
Mismatch wavelength (ML)	4.5	2.5	2.3	8.0	3.0
Transition length (TL) (mm)	40	90	72	31	70
Maximum matching fraction (MFMAX)	0.98	0.99	0.99	0.99	0.99
Minimum matching fraction (MFMIN)[a]	−0.02	−0.06	0	−0.09	0
Standard deviation, σ_a	0.65	0.42	0.64	0.71	0.47
Fractal dimension, D_f	2.64	2.69	2.78	2.67	2.61
Anisotropy in fractal dimension of the aperture, $A_a\sigma$	1.02	1.07	0.76	1.01	0.98
Arbitrary parameters					
Arithmetic mean aperture $<z_a>_a$ (mm)	1.71	0.82	1.40	1.55	1.29
Harmonic mean aperture $<z_a>_h$ (mm)	0	0	0	0	0
Geometric mean aperture $<z_a>_g$ (mm)	0	0	0	0	0
Dual mean of fracture aperture in *x*-direction (mm)	1.33	0.66	1.11	1.08	0.96
Dual mean of fracture aperture in *y*-direction (mm)	1.34	0.70	1.22	1.11	1.09

Harmonic and geometric means of the fracture are 0 because at least one touching point exists, where the aperture is 0. *a* = granite, *b* = syenite, *c* = gabbro, *d* = sandstone, *e* = granodiorite.

[a] The theory presumes the minimum value for the minimum matching fraction (MFMIN) to be zero. Negative values were found in the process of measurements and characterization may mean the theory does not reflect fracture features perfectly. Authors have no reasonable explanations to these negative values.

meters, grouped as (i) surface, (ii) fracture and (iii) arbitrary are discussed in detail in Ogilvie et al. [13]. The fracture apertures have log-normal distributions (Fig. 4). This is common for rough fracture apertures (e.g., [22]). As can be seen from the data, the fracture apertures increase with fractal dimension as the roughness of the fracture surfaces increases [13]. Non-fractal features were not observed. A dual mean aperture (combination of geometric and arithmetic means) has also been used which removes the difficulty of zero calculated aperture for rock apertures that touch at a single point, and enables prediction of hydraulic aperture from the Local Cubic Law. This is reported in a sister paper.

In SynFrac, the matching properties of the fractures were calculated using the Brown [4] method, Glover et al. [8,9] method and our improved method of controlling the degree of fracture surface correlation with wavelength [11,13]. These synthetic fracture apertures were then exported to ParaFrac for checking, analysis and production of power spectral density ratio plots. These plots in Fig. 5 show the differences between the matching properties of the real rock fractures and those predicted by these models. The matching properties of real rock fractures are closest to the Glover et al. [8,9] and the new model [13] and quite unlike those predicted by the Brown [4] model. In fact, the Brown [4] model gives the smallest values of fracture aperture and can significantly underestimate it (Table 1). The rate of change of matching around the matching wavelength is described by the transition length (mm). In general, this value is higher for those surfaces with lower fractal dimension e.g., the syenite (fracture) has a transition length of 90 compared to a value of 31 for the sandstone fracture.

5. Discussion

Spectral analyses show that rough surfaces are fractal or self-affine in nature (e.g., [4,8,9,13,22,27,28]).

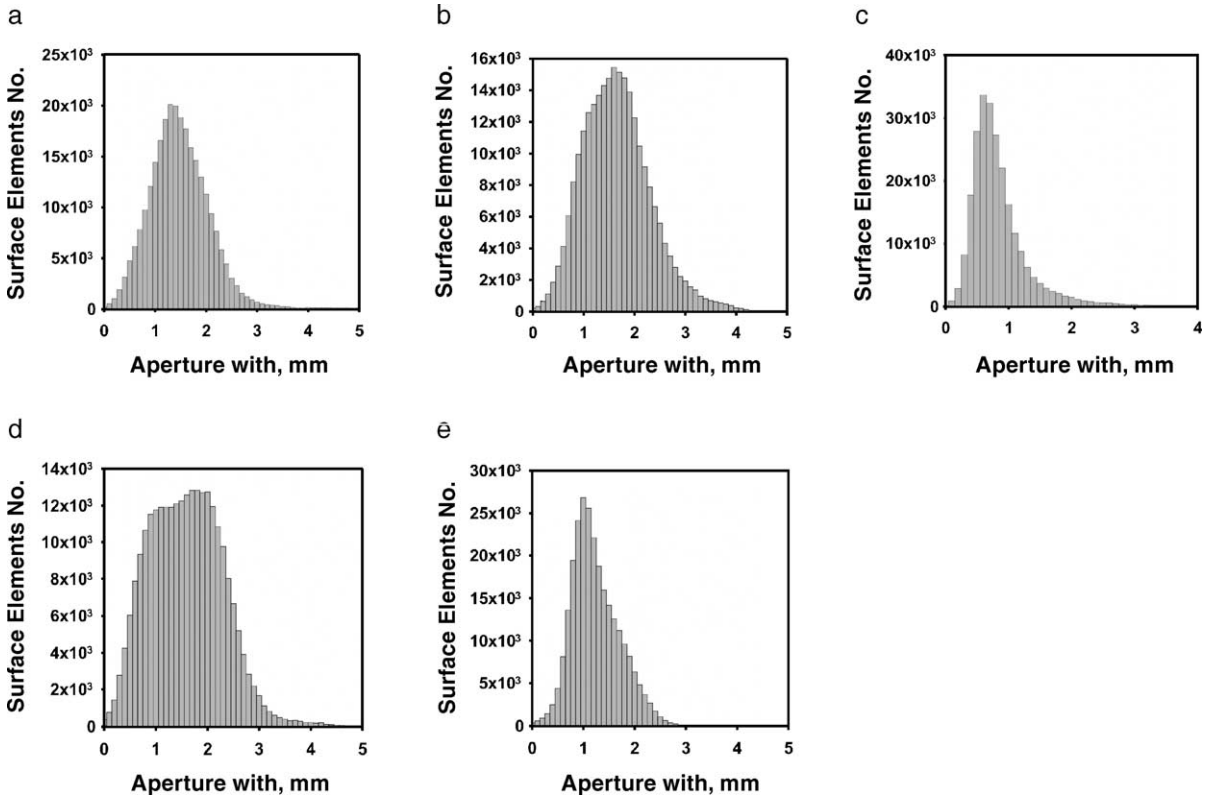

Fig. 4. Basic statistics for real (rough) fracture apertures; all apertures have log-normal shapes, (a) granite, (b) syenite, (c) gabbro, (d) sandstone and (e) granodiorite.

This means that surface irregularities are present at all scales, with longer wavelength irregularities having larger amplitude and contributing more to overall roughness than short wavelength features [4]. Various power laws reviewed in this paper describe the change of roughness with scale. The Brown [4] model indicates that there is not an abrupt transition between these scales when defining a mismatch length (ML) scale between matched behaviour at large scales and independent behaviour at small scales. However, it is unlikely that such a simple model can describe the complex matching properties of real rock fractures.

To investigate this, synthetic fractures created using various matching models have been useful. Although these fractures have geometrical parameters that are tuned to those of the natural fracture, their physical topography may be, and in general is, distinct. Each synthesis process is fully deterministic, so re-use of the same pair of random number seeds (with the same geometrical parameters) produces exactly the same two fracture surfaces and the resulting aperture. Synthetic fractures are quick and easy to create, and once the initial parameters are known any number of different fractures with the same properties may be created. For example, Glover et al. [7,9] used a synthetic modelling technique to show that flow modelling at cm-scale can be applied directly to flow at 100 m scale in a geothermal field in Japan and that the effect of fracture roughness can be accounted for by a single parameter. Flow modelling on a suite of such fractures allows the mean flow behaviour to be judged, which is representative of that type of fracture. Also, the scatter in the flow modelling results represents the range of expected values for all fractures with the given geometrical parameters [13].

Although fracture surfaces display a Fourier spectrum with power law behaviour over the full range of length scales extending to the sample size, local apertures have a spectrum that is power-law up to a critical length scale, the mismatch wavelength [ML], which flattens out at large scales [17]. Meheust and Schmittbuhl [15] expect this scale to have a strong impact upon flow, controlling channelling effects and the related hydraulic behaviour at the fracture scale. The Brown [4] and Glover et al. [8,9] definitions of mismatch wavelength [ML] attempt to measure the minimum wavelength at which the matching begins. Brown [4] used two pragmatic definitions for how this parameter

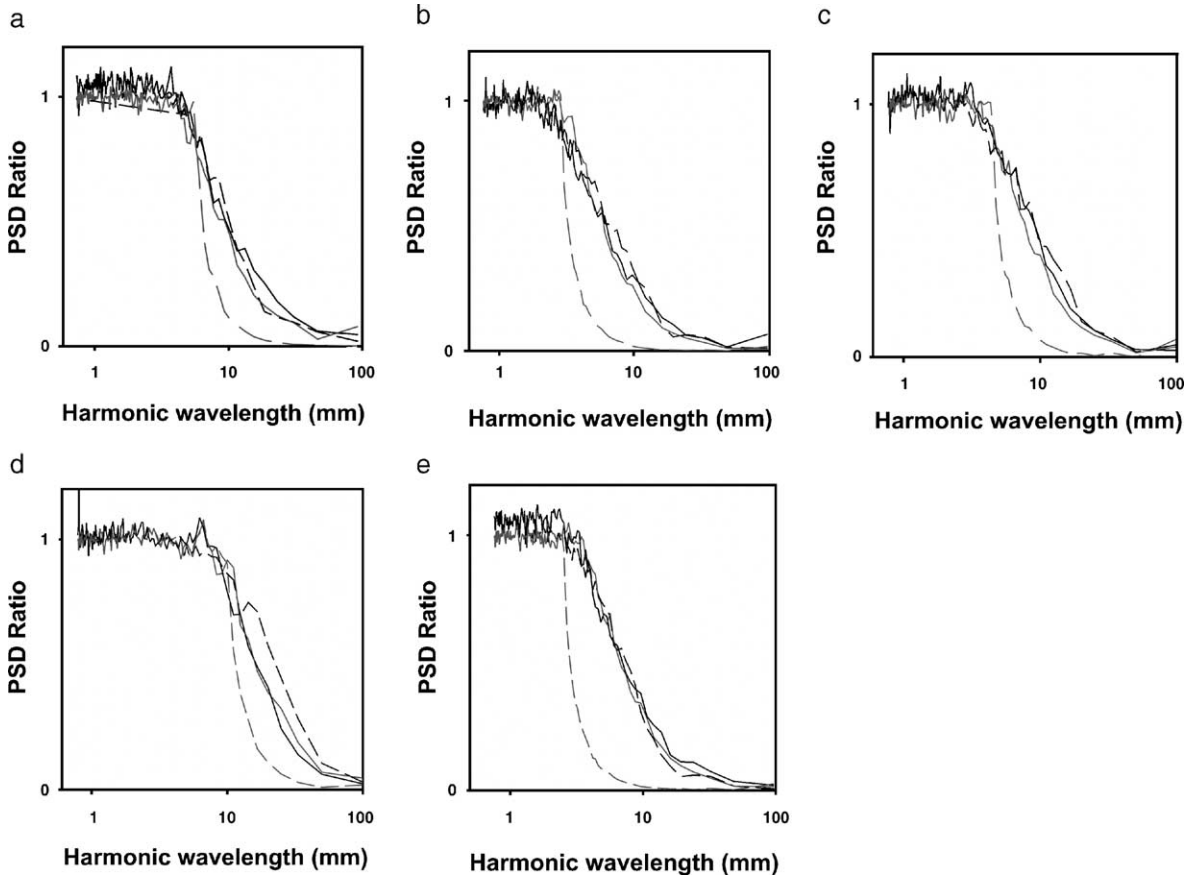

Fig. 5. Power spectral density ratio (PSDR) plots for derivation of fracture parameters (a) granite, (b) syenite, (c) gabbro, (d) sandstone and (e) granodiorite. Natural fracture (——), New model (- - - -), Glover et al. model (—–—), Brown model (– – –).

can be derived from real rock data. Both are based on a plot of the ratio of the PSD of the aperture to the PSD of one of the fracture surfaces (or their mean PSD) as a function of wavenumber. This curve, the $PSDR_{Brown}$, varies from about 2.0 at high wavenumbers, where no matching occurs, to values less than unity but greater than zero at low wavenumbers, where matching is developed. One of the Brown definitions of the mismatch wavelength was that wavelength where the $PSDR_{Brown}$ curve visibly deviates from its value (about 2.0) at high wavenumbers. This is clearly a qualitative and ambiguous definition (Fig. 1). The other Brown [4] definition of the mismatch wavelength was that wavelength where $PSDR_{Brown}=1.0$, which is a much more robust definition. The first of these values can be approximated from the PDSR curve used in this work because it corresponds to the wavelength where the PSDR curve visibly deviates from its unity value at high wavenumbers, and if the value of the PSDR is less than unity at the highest wavenumber in the data set, it may be said to lie at a larger wavenumber than occurs in the data set. The second of the Brown [4] definitions of mismatch wavelength can be obtained from the PDSR curve used in this work because it corresponds to the wavelength where the $PSDR=0.5$ providing the Fourier components of both surfaces are approximately equal at any given wavenumber. Glover et al. [8,9] used the two Brown [4] definitions of mismatch wavelength together with a third definition based upon the fitting of a linear regression to the $PSDR_{Brown}$ plot data for the wavenumbers where matching is gradually developing. This Glover et al. [8,9] definition of mismatch wavelength is the wavelength that corresponds to a wavenumber where the linear regression line fitted through the tail of the $PSDR_{Brown}$ curve intersects the line $PSDR_{Brown}=2.0$. Consequently, it should lie between the two definitions of Brown, as shown schematically in Fig. 1b.

The Brown [4] model underestimates fracture aperture and the Glover et al. [8,9] model slightly over predicts it as they use restricted parameters to control the fracture aperture. This can be seen when plotting power spectral density ratios (PSDRs) from the aperture

and the sum of the PSDs of the two surfaces composing the fracture, as a function of wavelength for the samples (Fig. 5). Also, we know from analysis of real rocks that the change is not instantaneous, but gradual. The model of Glover et al. [8,9] went some way to account for this. They used independent surfaces up to a wavelength of half the mismatch wavelength (ML), (i.e., zero correlation between the two surfaces in Fig. 1), then increased the degree of matching (correlation) linearly to some maximum degree of matching defined at the largest wavelength possible for the fracture, i.e., the maximum matching fraction (MFMAX).

To account for the more complex matching behaviour of real rock fractures, we use four parameters, the mismatch wavelength (ML), and maximum matching fraction of Glover et al. [8,9] and two additional parameters, a minimum matching fraction (MFMIN), and a transition length (TL). The mismatch wavelength (ML) represents twice the wavelength lower than which there is no correlation between the two fracture surfaces, and twice the wavelength higher than which the degree of correlation begins to increase linearly until some maximum value of matching, expressed as a fraction of complete matching, that is defined at the largest wavelength of the model or the measurement. This is called the maximum matching fraction (MFMAX). The transition length (TL) describes how fast in wavelength space the matching develops. Variation of this parameter gives smooth transition between Brown [4] and Glover et al. [8,9] methods. Ogilvie et al. [13] show that the mean aperture of the synthetic fracture increases as the transition length increases up to 80 mm. As the transition length becomes comparable to the size of whole fracture (100 mm), further increasing of the transition length does not affect the fracture properties. A large transitional length (TL) causes considerable scattering of mean aperture values, because the correlation between long-wave harmonics with highest amplitude becomes random. The fractured syenite has the greatest transition length (TL) [13].

Consequently, the new definition of mismatch wavelength (ML) will always produce a ML greater than the Brown [4] or Glover et al. [8,9] values. It must be noted that the Glover et al. [8,9] model works well for these rocks, however, that cannot be guaranteed for all rocks, and will fail for some scales for even the same rocks due to the assumptions implicit in the model needed to reduce the number of controlling matching parameters. However, this model has a reduced parameter set due to assumptions that it makes (e.g., that matching is fully developed at long wavelengths and not developed at all at the shortest wavelengths in the sample). The advantage of our model is that the parameters used cover all variations of matching parameters. It also includes a refinement for generating partially correlated random numbers required for the simulation of statistically similar aperture distributions. This is important as the random numbers control the actual topographies of the two fracture surfaces, and therefore control the resulting aperture.

The new model cannot account for natural fractures with non-fractal geometries e.g., the distribution and size of step features on rock joints. Also, it does not handle interbedded or multiple lithologies, although it is clear that the change in lithology may affect all of the parameters that are used to characterise the fracture geometries and to make synthetic fractures. Also, displacements of a few microns can have a major effect on the nature of fracture aperture space [29]. This is out of the scope of the current work and in later publications we describe how the techniques used here are relatively easily modified to examine the effect of modelled shear displacement on fracture geometry and fluid flow (e.g., [30]).

The point at which “the fracture surfaces just touch” depends on both the scale (at least for scales less than the transition scale) and the load (due to asperity deformation) [18,31]. The fracture surfaces are assumed to just touch at one point. In nature, fracture surfaces approach until the contact area, generated by asperity crushing, is sufficient to withstand the normal pressure across the fracture. It would be useful to account for normal pressure across the fracture. This is however, difficult as one needs to know (i) the relevant normal pressure and (ii) the local small-scale strength of individual rock asperities and in its absence we have taken the pragmatic approach of one touching point. Previous approaches progressively overlapped the two rock surfaces and assumed that the area of the overlap was directly proportional to the normal pressure required to make the overlap happen (e.g., [9,32]). One assumes a mean rock strength per unit volume, which was the same for all types, geometries and minerals in each asperity whereas in reality weaker minerals at the apices of asperities will be weaker per unit volume than stronger minerals inside wider asperities. These deformations have been modelled in a more rigorous manner by Pyrak-Nolte and Morris [33].

6. Conclusions

Fractal models of rough surfaces have been shown to be reasonable representations of natural rock surfaces (e.g., [34]). Our new fractal model can completely

describe the variation of matching properties in natural rock fractures. It generalizes the method of Glover et al. [8,9] that describes that transition from completely uncorrelated to correlated fracture surfaces with increasing scale. To do this we have defined a mismatch wavelength (ML), the size of a transition zone (the transition length, TL) centred on the mismatch wavelength, a minimum matching fraction (MFMIN), a maximum matching fraction (MFMAX), and the shape of the function describing the transition. We introduce the use of Fourier analyses as a means of analysing the matching behaviour of fracture surfaces (in addition to determination of fractal dimension). The new definition of mismatch (ML) wavelength is a measure of the wavelength halfway between the largest wavelength at which minimum matching occurs and the smallest wavelength at which maximum matching occurs. The new model also includes a refinement for generating partially correlated random numbers (incorporating a position swapping algorithm).

It is important to demonstrate that the statistical description of the aperture distribution is sufficient to ensure that the simulated aperture fields have similar flow and transport properties. This is addressed in a sister paper.

Acknowledgements

This work is funded by the Natural Environmental Research Council of the UK, as part of the Micro-to-Macro Thematic Programme. We would like to thank Judith Christie and Colin Taylor for their technical assistance during this study.

References

[1] S.R. Ogilvie, P.W.J. Glover, The microstructure of deformation bands in relation to their petrophysical properties, Earth Planet. Sci. Lett. 193 (2001) 133–147.
[2] I. Neretnieks, T. Eriksen, P. Tahtinen, Tracer movement in a single fissure in granitic rock: some experimental results and their interpretation, Water Resour. Res. 18 (1982) 849–858.
[3] S.R. Brown, Fluid flow through rock joints: the effect of surface roughness, J. Geophys. Res. 92 (B2) (1987) 1337–1347.
[4] S.R. Brown, Simple mathematical model of a rough fracture, J. Geophys. Res. 91 (1995) 5941–5952.
[5] S.R. Brown, A. Caprihan, R. Hardy, Experimental observation of fluid flow channels in a single fracture, J. Geophys. Res. 103 (1998) 5125–5132.
[6] P.W.J. Glover, K. Matsuki, R. Hikima, K. Hayashi, Fluid flow in fractally rough synthetic fractures, Geophys. Res. Lett. 24 (14) (1997) 1803–1806.
[7] P.W.J. Glover, K. Hayashi, Modelling of fluid flow in rough fractures: application to the Hachimantai geothermal HDR test site, Phys. Chem. Earth 22 (1–2) (1997) 5–11.
[8] P.W.J. Glover, K. Matsuki, R. Hikima, K. Hayashi, Synthetic rough fractures in rocks, J. Geophys. Res. 103 (1998) 9609–9620.
[9] P.W.J. Glover, K. Matsuki, R. Hikima, K. Hayashi, Fluid Flow in synthetic rough fractures and application to the Hachimantai geothermal HDR test site, J. Geophys. Res. 103 (1998) 9621–9635.
[10] C.E. Renshaw, S.R. Dadakis, Measuring fracture apertures: a comparison of methods, Geophys. Res. Lett. 27 (2000) 289–292.
[11] E. Isakov, P.W.J. Glover, S.R. Ogilvie, Use of synthetic fractures in the analysis of natural fracture apertures, Proceedings of the 8th European Congress for Stereology and Image Analysis, Image Analysis and Stereology, vol. 20 (2), 2001 (Sept.), pp. 366–371 SUPPL. 1.
[12] E. Isakov, S.R. Ogilvie, C.W. Taylor, P.W.J. Glover, Fluid flow through rough fractures in rocks: I. High resolution aperture determinations, Earth Planet. Sci. Lett. 191 (2001) 267–282.
[13] S.R. Ogilvie, E. Isakov, C.W. Taylor, P.W.J. Glover, Characterisation of rough-walled fractures in crystalline rocks, Spec. Publ.-Geol. Soc. Lond. 214 (2003) 125–141.
[14] D.J. Brush, N.R. Thomson, Fluid flow in synthetic rough-walled fractures: navier-stokes, stokes, and the local cubic law simulations, Water Resour. Res. 39 (2003) 5-1–5-15.
[15] Y. Meheust, J. Schmittbuhl, Scale effects related to flow in rough fractures, Pure Appl. Geophys. 160 (2003) 1023–1050.
[16] S.R. Brown, C.H. Scholz, Broad bandwidth study of the topography of natural rock surfaces, J. Geophys. Res. 90 (1985) 12575–12582.
[17] S.R. Brown, R.L. Kranz, B.P. Bonner, Correlation between the surfaces of natural rock joints, Geophys. Res. Lett. 13 (1986) 1430–1433.
[18] S.R. Brown, C.H. Scholz, Closure of rock joints, J. Geophys. Res. 91 (1986) 4939–4948.
[19] M.W. Jessel, S.J.D. Cox, P. Schwarze, W.L. Power, The anisotropy of roughness measured using a digital photogrammetric technique, in: M.S. Ameen (Ed.), Fractography: Fracture Topography as a Tool in Fracture Mechanics and Stress Analysis, Geol. Soc. Spec. Publ., vol. 92, 1995, pp. 27–37.
[20] F. Plouraboue, P. Kurowski, J.-P. Hulin, S. Roux, J. Schmittbuhl, Aperture of rough cracks, Phys. Rev., E 51 (1995) 1675–1685.
[21] A.A. Keller, P.V. Roberts, M.J. Blunt, Effect of fracture aperture on the dispersion of contaminants, Water Resour. Res. 35 (1) (1999) 55–63.
[22] W.L. Power, T.E. Tullis, The contact between opposing fault surfaces at Dixie Valley, Nevada, and implications for fault mechanics, J. Geophys. Res. 97 (1992) 15425–15435.
[23] S.R. Ogilvie, E. Isakov, P.W.J. Glover, C.W. Taylor, A new high resolution optical method for obtaining the topography of fracture surfaces in rocks, Image Anal. Stereol. 21 (1) (2002) 61–66.
[24] W.L. Power, T.E. Tullis, S.R. Brown, G.N. Boitnott, C.H. Scholz, Roughness of natural fault surfaces, Geophys. Res. Lett. 14 (1987) 29–32.
[25] A.R.H. Swan, M. Sandilands, Introduction to Geological Data Analysis, Blackwell Science, 1995. 446 pp.
[26] D. Saupe, Algorithms for random fractals, in: H-O. Peitgen, D. Saupe (Eds.), The Science of Fractal Images, Springer-Verlag, New York, 1988, pp. 71–136.
[27] S. Brown, H. Stockman, S. Reeves, Applicability of Reynolds equation for modeling fluid flow between rough surfaces, Geophys. Res. Lett. 22 (1995) 2537–2540.

[28] S.R. Brown, Measuring the dimension of self-affine fractals: example of rough surfaces, in: C. Barton, P.R. La Pointe (Eds.), Fractals in the Earth Sciences, Plenum Press, New York, 1995.
[29] N.E. Odling, Natural fracture profiles, fractal dimension and joint roughness coefficient, Rock Mech. Rock Eng. 27 (3) (1994) 135–153.
[30] I.W. Yeo, R.W. Zimmerman, M.H. deFreitas, Effect of shear displacement on the aperture and permeability of a rock fracture, Int. J. Rock Mech. 35 (1998) 1051–1070.
[31] R.W. Zimmerman, D.W. Chen, N.G.W. Cook, The effect of contact area on the permeability of fractures, J. Hydrol. 139 (1992) 79–96.
[32] P.W.J. Glover, K. Matsuki, R. Hikima, K. Hayashi, Characterizing rock fractures using synthetic fractal analogues, Geotherm. Sci. Technol. 6 (1999) 83–112.
[33] L.J. Pyrak-Nolte, J.P. Morris, Single fractures under normal stress: the relation between fracture specific stiffness and fluid flow, Int. J. Rock Mech. Min. Sci. 37 (2000) 245–262.
[34] S.R. Brown, C.H. Scholz, Closure of random elastic surfaces in contact, J. Geophys. Res. (1985) 5531–5545.